Egyptian Journal of Petroleum (2013) 22, 493–499

Egyptian Petroleum Research Institute

Egyptian Journal of Petroleum

www.elsevier.com/locate/egyjp
www.sciencedirect.com

FULL LENGTH ARTICLE

Fabrication and characterization of nanoclay composites using synthesized polymeric thiol surfactants assembled on gold nanoparticles

E.M.S. Azzam [a,*], S.M. Sayyah [b], A.S. Taha [b]

[a] Applied Surfactants Laboratory, Petrochemicals Department, Egyptian Petroleum Research Institute, Elzhoor, Nasr City, 11727 Cairo, Egypt
[b] Polymer Research Laboratory, Chemistry Department, Faculty of Science, Beni-Suef Branch, Cairo University, 62111 Beni-Suef City, Egypt

Received 6 September 2012; accepted 17 October 2013
Available online 8 December 2013

KEYWORDS
Nanoclay composites;
Polymeric thiol surfactants;
Gold nanoparticles

Abstract In the present work, the nanoclay composites were fabricated using the synthesized poly 6-(3-aminophenoxy) hexane-1-thiol, poly 8-(3-aminophenoxy) octane-1-thiol and poly 10-(3-aminophenoxy) decane-1-thiol surfactants with gold nanoparticles. The polymeric thiol surfactants were first assembled on gold nanoparticles and then impregnated into the clay matrix. Different spectroscopic and microscopic techniques such as X-ray diffraction (XRD), Scanning electron microscope (SEM) and Transmission microscope (TEM) were used to characterize the fabricated nanoclay composites. The results showed that the polymeric thiol surfactants assembled on gold nanoparticles are located in the interlayer space of the clay mineral and affected the clay structure.

1. Introduction

The intercalated nanocomposites can be used in different scientific areas. The applications include their use for fabrication of paper, paints, and inks, for optical, electrical, catalytic, thermal, and mechanical industries, for ceramic raw material, cosmetics, medicines, and so forth [1–5]. Nanoclays for plastic composites refer to a category of clay minerals with a specialized structure that was characterized by plate morphology. The most widely used nanoclay for plastic composite is modified montmorillonite clay. Montmorillonite is a 2-to-1 layered smectite clay mineral with a platy structure. Each layer has 2 tetrahedral sheets containing an octahedral sheet between them. Individual platelet thicknesses are just 1 nm, but surface dimensions are generally 300 to more than 600 nm, resulting in an unusually high aspect ratio. Hundreds or thousands of these layers are stacked together with vander Waals forces to form clay particles [6]. Polymer-layered silicate nanocomposites have recently gained a great deal of attention because they offer a great potential to provide superior properties when compared to pure polymers and conventional filled

* Corresponding author.
E-mail address: eazzamep@yahoo.com (E.M.S. Azzam).
Peer review under responsibility of Egyptian Petroleum Research Institute.

ELSEVIER Production and hosting by Elsevier

1110-0621 © 2013 Production and hosting by Elsevier B.V. on behalf of Egyptian Petroleum Research Institute.
Open access under CC BY-NC-ND license. http://dx.doi.org/10.1016/j.ejpe.2013.11.011

composites. The properties include high dimensional stability, high heat deflection temperature, reduced gas permeability, improved flame retardance, and enhanced mechanical properties [7–9]. Since the advent of nylon-6/montmorillonite nanocomposites developed by Toyota Motor Co., the studies on polymer/clay nanocomposites have been successfully extended to many other polymer systems [8]. Smectite clays have increasingly attracted research interests as hosts for the preparation of nanoparticle/clay nanocomposites in the past decade due to the possibility to retain the small size and various shapes of the nanoparticles after intercalation and further industrial exploitation of the composite [10]. The unique physicochemical properties of smectite clays are the result of their extremely small crystal size, variation of the internal chemical composition, structural characteristics caused by chemical factors, large cation exchange capacity, large chemically active surface area, variation in types of exchangeable ions and surface charge, and interactions with inorganic and organic liquids. Clay minerals have a very strong swelling and adsorption capacity, which is particularly interesting for the impregnation of catalytically active noble metals in the interlamellar space of clay [11]. Several methods were reported in the literature for the preparation of nanoparticle/clay (especially SiO2-based clays) composites [12–18]. The impregnation of preformed nanoparticles into a clay matrix can offer a new and facile procedure for nanometal/clay composite fabrication where the size and morphology of the nanoparticles are better controlled by separate and mostly standard preparation steps [19]. The past decade has seen a great upsurge in research on polymer–clay nanocomposites, because these materials can offer enhanced fire, mechanical and barrier properties compared to polymer composites containing traditional fillers. Work has been conducted on a wide variety of polymers, including thermoplastics, such as styrenics, polyolefins, etc. and thermosetting materials, such as epoxy resins and phenolics [20]. Here in, we investigated the fabrication of nanoclay composites using the synthesized polymeric thiol surfactants and gold nanoparticles. The fabricated nanoclay composites were characterized using different experimental techniques such as X-ray diffraction (XRD), Scanning electron microscope (SEM) and Transmission microscope (TEM). In addition, we studied the effect of the synthesized polymeric surfactants and the gold nanoparticles on the properties of the prepared nanoclay composites.

2. Materials and methods

2.1. Materials

2.1.1. Synthesize of the polymeric thiol surfactants

The polymeric thiol surfactants under investigation were synthesized according to the previous publication [21]. The chemical structure (Scheme 1) of the synthesized poly 6-(3-amino phenoxy) hexane-1-thiol, poly 8-(3-amino phenoxy) octane-1-thiol and poly 10-(3-amino phenoxy) decane-1-thiol surfactants was confirmed using FTIR and thermal gravimetric analysis (TGA).

2.1.2. Synthesize of gold nanoparticles (AuNPs)

Gold nanoparticles (AuNPs) of ~25 nm size were prepared by the reduction of tetrachloroauric acid ($HAuCl_4$) using

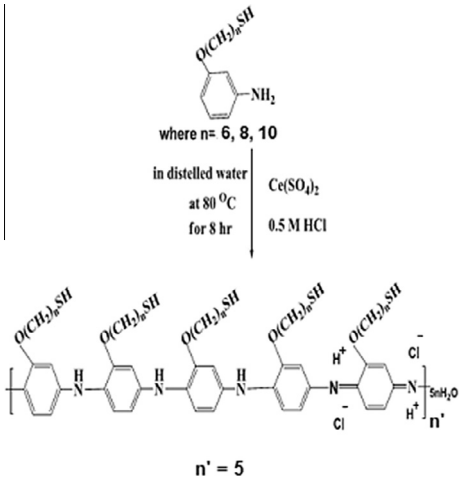

Scheme 1 Chemical structure of the synthesized polymeric surfactants (C6, C8 and C10).

tri-sodium citrate ($Na_3C_6H_5O_7$). 2 ml of tetrachloroauric acid solution (1%) was heated to boiling temperature then 2.5 ml of tri-sodium citrate solution (1%) was added slowly and stirred until the color changed to winy red. All solutions were prepared using pure distilled water which was obtained by passing twice-distilled water through a Milli-Q system. The formation of gold nanoparticles colloidal solution was characterized using the TEM and UV analysis as shown in Figs. 1 and 2 [22].

2.1.3. Assembling of the synthesized polymeric surfactants on gold nanoparticles

The synthesized surfactants were assembled onto the surface of gold nanoparticles by mixing 20 ml of the prepared AuNPs solution with 5 ml of 1×10^{-5} M from surfactant solution and stirred at room temperature for 24 h until the solution became colorless [23].

2.1.4. Synthesize of clay nanopowder

The nanopowder form of the clay was prepared using RETSCH Planetary Ball Mills Type PM 400. The clay sample was milled using the ball mill at a speed of 150 rpm for 8 h [24].

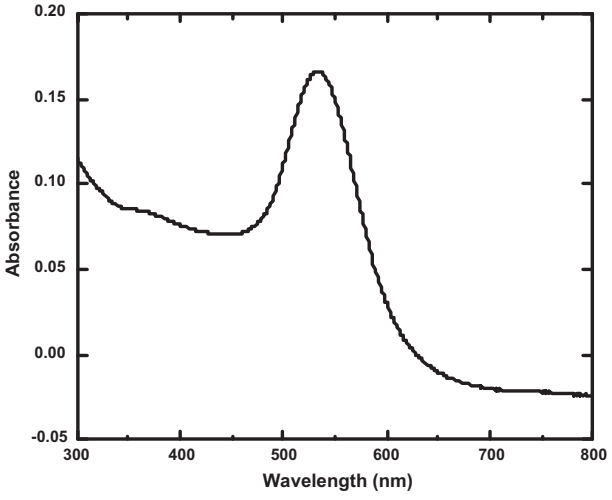

Figure 1 UV spectra for the AuNPs solution.

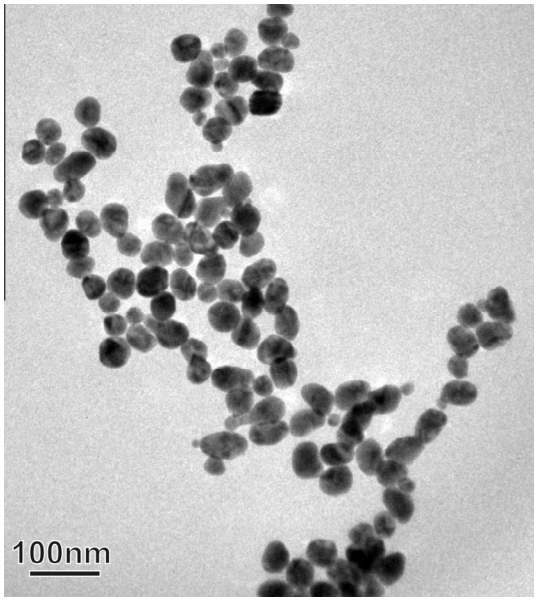

Figure 2 TEM of the gold nanoparticles (AuNPs) solution.

2.1.5. Fabrication of the nanoclay composite with AuNPs

The fabrication of the nanoclay composites using AuNPs solution was carried out as shown in the previous publication [19]. A total of 1 g of the clay nanopowder was dispersed in 250 ml of water for swelling for 48 h. The clay nanopowder was then separated by centrifugation and transferred into the suspension solution (50 ml) of AuNPs. The mixture was stirred for 24 h. The precipitate was separated by centrifugation, washed with water, and dried under vacuum overnight.

2.1.6. Fabrication of the nanoclay composite with nanostructure of the synthesized polymeric surfactants (C6–C10) assembled on AuNPs

The fabrication of the nanoclay composites using the synthesized polymeric surfactant assembled on gold nanoparticles was carried out as shown in the above step as follows: A total of 1 g of the clay nanopowder was dispersed in 250 ml of water for swelling for 48 h. The clay nanopowder was then separated by centrifugation and transferred into the suspension solution (50 ml) of the polymeric surfactant assembled on gold nanoparticles in order to prepare the clay nanocomposite with the nanostructure of these polymeric surfactants. The mixture was stirred for 24 h. The precipitate was separated by centrifugation, washed with water, and dried under vacuum overnight [19].

2.2. Methods

2.2.1. X-ray diffraction (XRD)

X-ray diffraction patterns were recorded with a Pan Analytical Model X'Pert Pro, which was equipped with CuKα radiation (λ = 0.1542 nm), Ni-filter and general area detector. The diffractograms were recorded in the 2θ range of 0.5–10 with step size of 0.02 and a step time of 0.605.

2.2.2. Scanning electron microscope (SEM)

Scanning electron microscope (HR-SEM) data for the nanostructure of the prepared samples in this work were obtained using SEM model Oxford instrument INCA/Sight 40 kV. The measurements were carried out at the National Research Centre.

2.2.3. Transmission electron microscope (TEM)

A convenient way to produce good TEM samples is to use copper grids. A copper grid was pre-covered with a very thin amorphous carbon film. To investigate the prepared samples, small droplets of the suspended solution for each sample were placed on the carbon-coated grid. A photographic plate of the transmission electron microscopy (Type JEOL JEM-1230 operating at 120 kV attached to a CCD camera) was employed in the present work to investigate the nanostructure of the prepared samples.

3. Results and discussion

3.1. X-ray diffraction (XRD)

XRD patterns of the clay nanopowder, clay nanocomposite with AuNPs and the clay nanocomposite with the nanostructures of the synthesized polymeric surfactants with AuNPs are represented in Fig. 3(a–e). Fig. 3(a) shows the XRD pattern of the clay nanopowder, the shift to lower 2θ values of the (0 0 1) and (0 0 2) reflections corresponding to Na^+-montmorillonite can be explained by swelling in the inter lamellar space of the clay mineral as represented by Belova et al. [19]. The results in Fig. 3(b) illustrate the XRD peaks of the nanoclay composite loaded with AuNPs. It was noticed that the samples have high intensity sharp peak corresponding to the (1 1 1) plane. In addition, the XRD pattern in Fig. 3(b) shows four peaks, the mean peak at $2\theta = 29.9^{o}$ corresponds to (1 1 0) and the other three slightly weak peaks at $2\theta = 44.4^{o}$, 64.8^{o}, and 77.9^{o} correspond to the (2 0 0), (2 2 0) and (3 1 1) planes of the cubic Au crystal, respectively. The XRD patterns in Fig. 3(c–e) for the clay nanocomposite with the nanostructures of the synthesized polymeric surfactants with AuNPs show some additional peaks to those that appeared in the Fig. 3(a and b) which is related to the presence of the synthesized polymeric surfactants (C6–C8) assembled on AuNPs. The results from Fig. 3(c–e) can confirm the formation of the clay nanocomposite with the nanostructures of the synthesized polymeric surfactants.

3.2. Scanning electron microscopy (SEM)

The SEM technique was used to investigate the surface morphologies of the prepared samples. The surface morphologies of the clay nanopowder, the fabricated clay nanocomposite with AuNPs and the fabricated clay nanocomposite with the nanostructure of the synthesized polymeric surfactants with AuNPs are shown in Fig. 4(a–e). The structures of the clay nanopowder and the fabricated clay nanocomposite with AuNPs are indicated in Fig. 4(a and b) shows a massive layered structure with some large flakes and some inter layer spaces. A comparison between the SEM images in Fig. 4(a and b), it is noticed that nearly the same surface morphologies are seen with the exception that the inter layer spaces are decreased in Fig. 4(b). This may be related to the impregnation of the AuNPs between the clay layers. The SEM images of

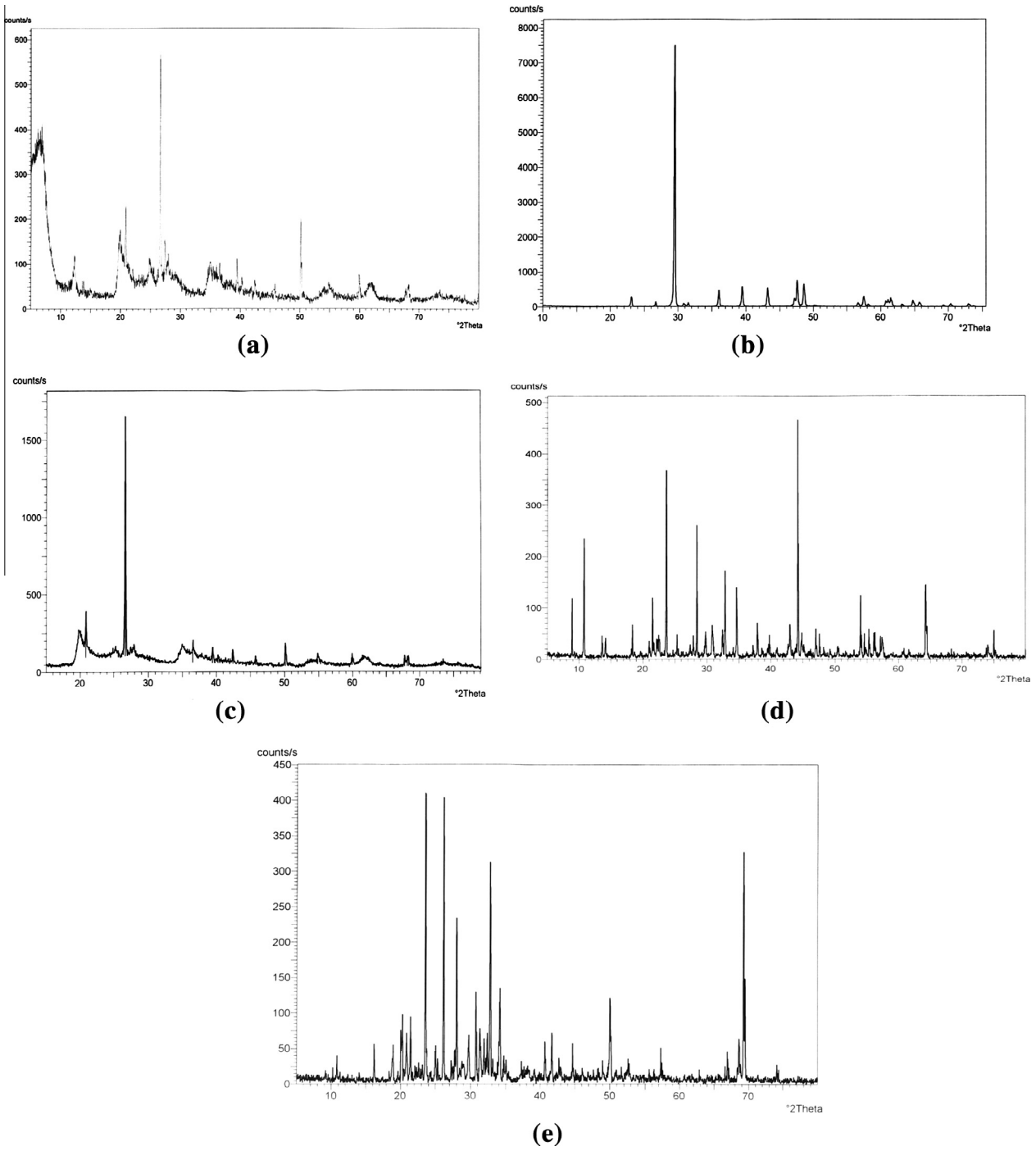

Figure 3 XRD patterns of the clay nanopowder (a), the clay nanocomposite with AuNPs (b), the clay nanocomposite with the nanostructure of C6 polymeric surfactant assembled on AuNPs (c), the clay nanocomposite with the nanostructure of C8 polymeric surfactant assembled on AuNPs (d) and the clay nanocomposite with the nanostructure of C10 polymeric surfactant assembled on AuNPs (e).

the fabricated clay nanocomposite with the nanostructure of the synthesized polymeric surfactants assembled on AuNPs in Fig. 4(c–e) show different surface morphologies than that of the clay nanopowder and clay nanocomposite with AuNPs. It is noticed that the inter layer spaces are more decreased in Fig. 4(c–e) which indicate the impregnation of the nanostructure of the polymeric surfactants between the clay layers. In addition the SEM images in Fig. 4(c–e) show that these inter layer spaces decrease as the alkyl chain length of the synthesized polymeric surfactants increased from C6 to C10.

3.3. Transmission electron microscope (TEM)

In this study the TEM technique is used for further investigation of the fabricated clay nanocomposite with AuNPs and with the nanostructures of the synthesized polymeric

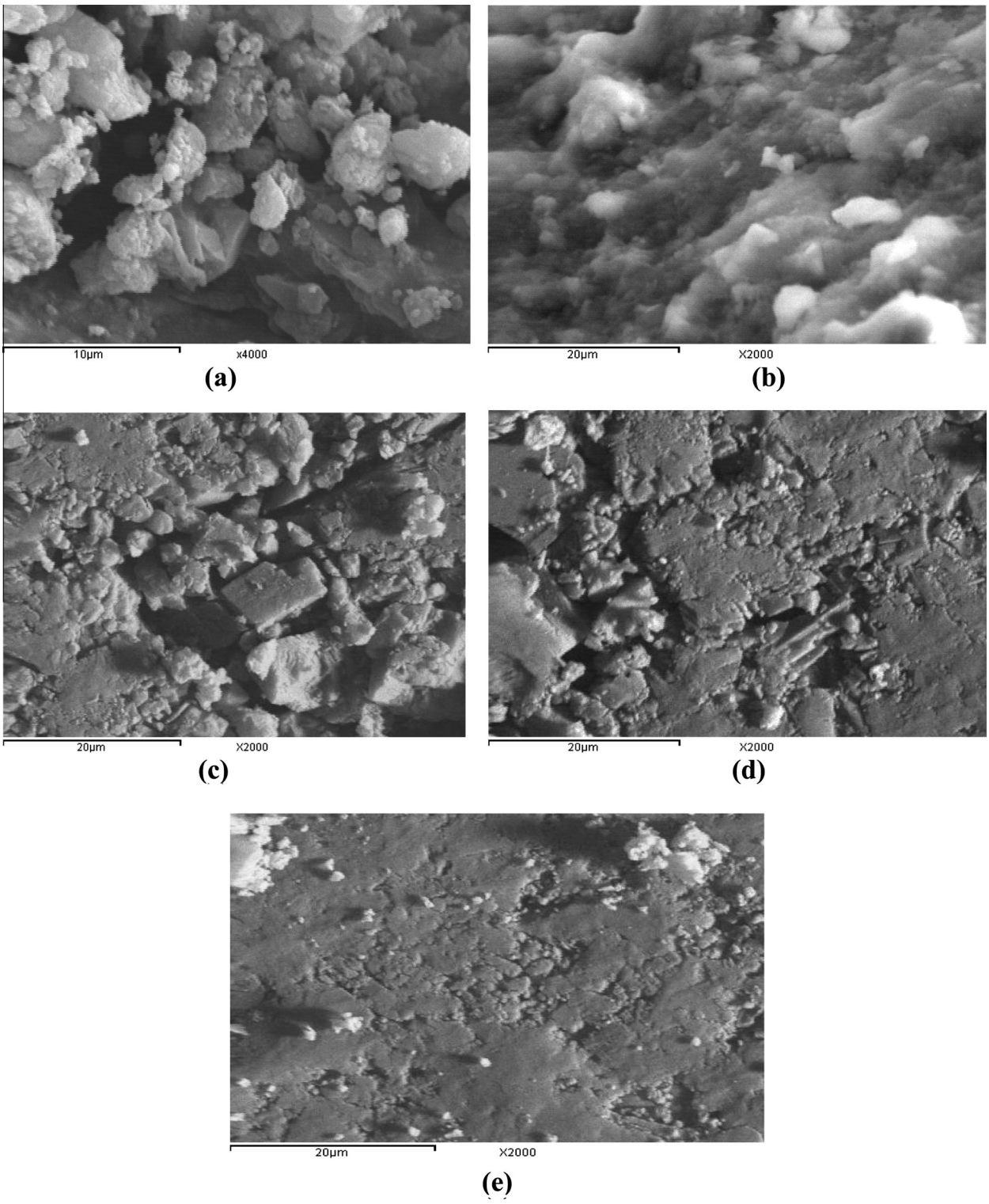

Figure 4 SEM images of the clay nanopowder (a), the clay nanocomposite with AuNPs (b), the clay nanocomposite with the nanostructure of C6 polymeric surfactant assembled on AuNPs (c), the clay nanocomposite with the nanostructure of C8 polymeric surfactant assembled on AuNPs (d), and the clay nanocomposite with the nanostructure of C10 polymeric surfactant assembled on AuNPs (e).

surfactants assembled on AuNPs. The TEM images of the clay nanopowder, clay nanocomposite with AuNPs and clay nanocomposite with the nanostructures of the synthesized polymeric surfactants assembled on AuNPs are presented in Fig. 5a–e. The TEM image in Fig. 5a demonstrates the typical structure of the montmorillonite clay image. It can be noticed from this image that there is a homogeneous distribution of the clay flakes. The TEM images of the clay nanocomposite

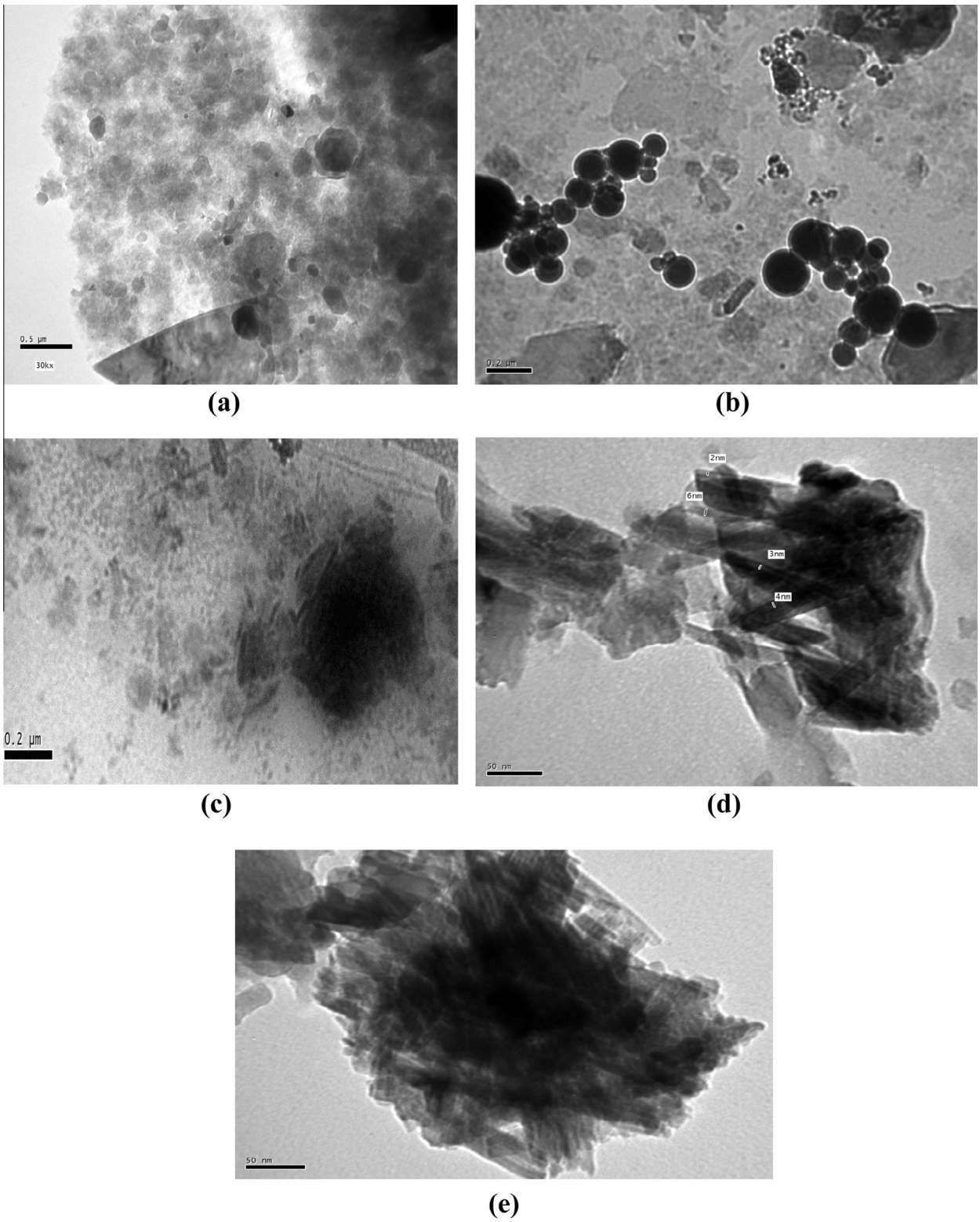

Figure 5 TEM images of the clay nanopowder (a), the clay nanocomposite with AuNPs (b), the clay nanocomposite with the nanostructure of C6 polymeric surfactant assembled on AuNPs (c), the clay nanocomposite with the nanostructure of C8 polymeric surfactant assembled on AuNPs (d) and the clay nanocomposite with the nanostructure of C10 polymeric surfactant assembled on AuNPs (e).

presented in Fig. 5b show a homogenous loading of the gold nanoparticles inside the clay matrix. Comparing the TEM micrographs in Fig. 5(a and b) confirmed the formation of the clay nanocomposite with the AuNPs. In addition, the TEM images in Fig. 5(c–e) shows the distribution of nanostructure of the synthesized polymeric surfactants assembled

on AuNPs within the inter layer spaces of clay which is compatible with the XRD and SEM results in this work and confirm the formation of the clay nanocomposite . It is clear from the TEM images in Fig. 5(c–e) that as the alkyl chain length of the polymeric surfactants increases from C6 to C10 the filling of the inter layer spaces of clay by the nanostructures of these polymeric surfactants increases.

References

[1] C.S.F. Gomes, Argilas. Aplicações na Indústria. Edição de autor. Aveiro. (2002) 338.
[2] C.C. Harvey, H.H. Murray, Appl. Clay Sci. 11 (1997) 285–310.
[3] H.H. Murray, Appl. Clay Sci. 17 (2000) 207–221.
[4] X. She, M. Flytzani-Stephanopoulos, J. Catal. 237 (2006) 79–93.
[5] A.K. Dutta, A.B. Chattopadhyay, K.K. Ray, J. Mater. Sci. Lett. 20 (2001) 917–919.
[6] F. Gao, Mater. Today 7 (2004) 50–55.
[7] E.P. Giannelis, Adv. Mater. 8 (1996) 29–35.
[8] M. Alexandre, P. Dubois, Mater. Sci. Eng. R28 (2000) 1–63.
[9] E.P. Giannelis, R. Krishnamoorti, E. Manias, Adv. Polym. Sci. 138 (1999) 107–147.
[10] J.W. Kim, S.G. Kim, H.J. Choi, M.S. Jhon, Macromol. Rapid Commun. 20 (1999) 450–452.
[11] R.E. Grim, Clay Mineralogy, McGraw-Hill Book Company, New York, 1968 (pp. 34–35).
[12] D. Manikandan, D. Divakar, T. Sivakumar, Catal. Commun. 8 (2007) 1781–1786.
[13] K.K.R. Datta, M. Eswaramoorthy, J. Mater. Chem. 17 (2007) 613–615.
[14] W. Chen, W. Cai, J. Colloid Interface Sci. 238 (2001) 291–295.
[15] A. Szücs, F. Berger, I. Dékány, Colloids Surf. A. 174 (2000) 387–402.
[16] M.J. Pérez-Zurita, G.J. Pérez-Quintana, Clay Clay Miner. 53 (2005) 528–535.
[17] S.M. Paek, J.U. Jang, S.J. Hwang, J.H. Choy, J. Phys. Chem. Solids 67 (2006) 1020–1023.
[18] S. Karaborni, B. Smit, W. Heidug, J. Urai, J. Sci. 271 (1996) 1102–1104.
[19] V. Belova, H. M??hwald, D.G. Shchukin, Langmuir 24 (2008) 9747–9753.
[20] W.H. Awad, G. Beyer, D. Benderly, W.L. Ijdo, P. Songtipya, M. del, M. Jimenez-Gasco, E.D. Manias, C.A. Wilkie, Polymer 50 (2009) 1857–1867.
[21] E.M.S. Azzam, A.F.M. El-Frarrge, D.A. Ismail, A.A. Abd-Elaal, JDST 32 (2011) 816–821.
[22] E.M.S. Azzam, Ch. Grunwald, A. Bashir, O. Shekhah, A.R.E. Alawady, A. Birkner, Ch. W?ll, Thin Solid Films 518 (2009) 387–391.
[23] E.M.S. Azzam, A.M. Badawi, A.R.E. Alawady, JDST 30 (2009) 540–547.
[24] E.M.S. Azzam, R.M. Sami, N.G. Kandile, Am. J. Biochem. 2 (2012) 29–35.